Journal of Ocean, Mechanical and Aerospace
-Science and Engineering-, Vol.3

January 20, 2014

Study of the Effect of Low Profile Vortex Generators on Ship Viscous Resistance

Yasser M. Ahmed[a, b,*], A. H. Elbatran[a], H. M. Shabara[a]

[a)]*Faculty of Mechanical Engineering, UniversitiTeknologi Malaysia, 81310, UTM , Skudai, Johor, Malaysia*
[b)]*Faculty of Engineering, Alexandria University, Egypt*

*Corresponding author: yasser@mail.fkm.utm.my

Paper History

Received: 18-December-2013
Received in revised form: 25-December-2013
Accepted: 29-December-2013

ABSTRACT

A study of the effect of the well-known aerodynamic device low profile vortex generators (VGs) on the viscous resistance of the DTMB 5415 ship hull form through the control of the ship boundary layer separation is performed using the finite volume code Ansys CFX. The tetrahedral unstructural grids have been used for meshing the different cases. Different types of VGs have been tested, but the study has forced on two main types of VGs. The effects of VGs on the ship viscous resistance and its components have been investigated for the different cases in this study, and comparisons between the various results have been made.

KEY WORDS: *Vortex Generator; Viscous Resistance; Aerodynamic Device.*

NOMENCLATURE

$C_{1\varepsilon}, C_{2\varepsilon}$	turbulence model constants
C_F	frictional resistance coefficient
C_{PV}	viscous pressure resistance coefficient
C_V	viscous resistance coefficient
G_k	turbulent kinetic energy due to mean velocity gradient
e	device chord length
f	device thickness or width
g	slots depth
h	device height
k	turbulent kinetic energy
ui	velocity components in the directions of xi =(x,y,z)
$\overline{u_i' u_j'}$	Reynolds stresses
ΔX_{VG}	distance between the VG trailing edge and the beginning of high pressure zone
z	device spacing in vertical direction
δ	boundary layer thickness
δ_{ij}	Kronecker delta
ε	dissipation rate of turbulence kinetic energy
υ_t	turbulent kinematic viscosity
$\sigma_k, \sigma_\varepsilon$	turbulence model constants
ρ	fluid density

1.0 INTRODUCTION

Flow separation control is a very important task for many industrial applications of fluid mechanics [1,2]. Controlling flow separation can result in a reduction of system resistance with consequence of energy conservation. Different methods can be used for controlling the flow separation, such as wall cooling, boundary layer suction or using vortex generators (VGs). There are numerous aerodynamic applications using VGs for reducing flow separation in internal and external flows.

Conventional passive VGs with $h/\delta \approx 1$ have been used to control flow separation in the boundary layer by increasing the

near wall momentum through the transfer of momentum from the free stream flow to the wall region. These VGs have been used to delay the separation of the boundary layer [3], to decrease resistance of aircrafts fuselages [4] and in other many applications. However, in some cases this type of VGs may cause a transferring of vehicle forward momentum into the unrecoverable turbulence in the wake region of the vehicle, which leads to an increase of the residual drag.

Kuethe [5] has investigated the effect of non-conventional VGs with h/δ of 0.27 and 0.42 on the boundary layer separation. These low profile VGs have the ability of reducing the area of velocity deficit in the wake region [5]. A lot of investigations and researches have been made to study the effect of the VGs height on the viscous flow control, and it has been found that the use of low profile VGs in the range of $0.1 \le h/\delta \le 0.5$ can provide good flow separation control [6] with lower drag of the VGs.

In aeronautical applications the low profile VGs may take different shapes and sizes, but the most common one is the vane type, while in marine field Odelal [7] provides a study for a range of different VGs geometries used for hydraulic and marine equipments. Odelal shows that investigations should be made before choosing a specific configuration of VGs for a particular application.

Indeed, there are few research works in the marine field of using VGs to control boundary layer separation; therefore this study is an attempt to investigate the effect of low profile VGs on the ship viscous flow. The model of the DTMB 5415 unit [8] has been chosen for this study as an example of ship hull form, and different shapes and sizes of VGs have been tested in this study. The effects on the viscous pressure resistance and the frictional resistance have been investigated with each type of the VGs.

2.0 GOVERNING FLOW EQUATIONS

The governing equations for the 3D steady incompressible turbulent flow adapted for this study are the continuity equation for mass conservation and Reynolds-Averaged Navier-Stokes equations for momentum transport. These equations can be written in Cartesian form as follows:

Continuity equation

$$\frac{\partial u_i}{\partial x_i} = 0 \tag{1}$$

Momentum transport equation

$$u_j \frac{\partial u_i}{\partial x_j} = -\frac{1}{\rho}\frac{\partial p}{\partial x_i} + \frac{\partial}{\partial x_j}\left[\upsilon\left(\frac{\partial u_i}{\partial x_j} + \frac{\partial u_j}{\partial x_i}\right)\right] + \frac{\partial}{\partial x_j}\left(-\overline{u_i' u_j'}\right) \tag{2}$$

Reynolds stresses

$$-\overline{u_i' u_j'} = \upsilon_t\left(\frac{\partial u_i}{\partial x_j} + \frac{\partial u_j}{\partial x_i}\right) - \frac{2}{3}k\delta_{ij} \tag{3}$$

Turbulence model equations

In this study the standard $k-\varepsilon$ turbulence model and the renormalization-group (RNG) $k-\varepsilon$ turbulence model [9] have been used for simulations. However, the best results have been obtained from using the standard $k-\varepsilon$ turbulent model. The equations of the standard $k-\varepsilon$ turbulence model can be expressed as follows:

$$\rho\frac{Dk}{Dt} = \frac{\partial}{\partial x_i}\left[\left(\mu + \frac{\mu_t}{\sigma_k}\right)\frac{\partial k}{\partial x_i}\right] + G_k - \rho\varepsilon \tag{4}$$

and

$$\rho\frac{D\varepsilon}{Dt} = \frac{\partial}{\partial x_i}\left[\left(\mu + \frac{\mu_t}{\sigma_\varepsilon}\right)\frac{\partial \varepsilon}{\partial x_i}\right] + C_{1\varepsilon}\frac{\varepsilon}{k}(G_k) - C_{2\varepsilon}\rho\frac{\varepsilon^2}{k} \tag{5}$$

3.0 DESCRIPTION OF DTMB 5415 HULL FORM AND VGs

Model DTMB 5415 (Fig. 1) was conceived as a preliminary design for a Navy surface combatant ca. 1980. The hull geometry includes both a sonar dome and transom stern. Propulsion is provided through twin open-water propellers driven by shafts supported by struts.

The principal dimensions of the DTMB 5415 are listed in Table 1 and the tests conditions are listed in Table 2 correspond to the model tests from the David Taylor Model Basin (DTMB) in Washington D.C. and the Istituto Nazionale per Studied Esperienze di Architettura Navale (INSEAN) in Rome, Italy. Both computations and experiments are conducted in the bare hull condition.

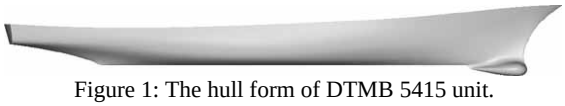

Figure 1: The hull form of DTMB 5415 unit.

Table 1: Principal dimensions of DTMB 5415 [8].

Length	142.037 m
Beam	17.983 m
Draft	6.179 m
Wet Surface Area	2976.7 m^2
Water Plane Area	1987.2 m^2
Displacement	12901.6 m^3
Block Coefficient	0.506

Table 2: Test conditions for the Model scale [8].

Scale Ratio	24.832
Length (L)	5.72 m
Draft (T)	0.248 m
Wet Surface Area (S)	4.861 m^2
Advance Velocity (U_0)	2.0637 m/s
Froude Number (Fn)	0.2755 m/s
Reynolds Number (Re)	1.26×10^7

In the current study vortex generators of delta shaped type and groves of slots shapes inthe ship hull form have been chosen for the investigations (Fig. 2). Moreover, other types of VGs have been tested, but the results of the previously mentioned types have been the best. The basic dimensions of the VGs used for every run in this study can be seen in Table 3. In fact, the vortex generators have been chosen based on aerodynamic studies, hydrodynamics studies and structural requirements [6], [10, 11].

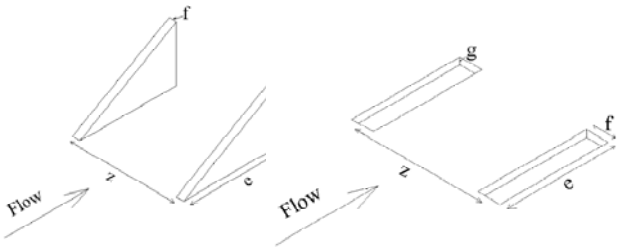

Figure 2(a) Geometry of delta shaped VGs, Figure 2(b) Geometry of hull slots

Table 3: Main specifications of the VGs used in this study.

Case	case1a case1b	case2a case2b	case3a case3b	Case4a Case4b	case5a case5b
VGs type	–	*Delta shaped vortex generators*			*Slots*
No. of VGs		*4*			*4*
h (m)		*0.0375*	*0.01875*		–
g (m)		–			*0.0005*
h/δ		*~ 0.2*	*~ 0.1*		–
e/h		*~1.733*			–
f/h		*0.133*			–
z/h		*~ 1.13*	*~ 2.26*	*~ 2.15*	–
e/g		–			*20*
z/g		–			*~ 84*
$\Delta X_{VG}/h$		*~ 1.2*	*~ 2.4*		–
$\Delta X_{VG}/g$		–			*~ 80*

In fact, it was found from the numerical simulations conducted in this research work that reducing or increasing the number of VGs than 4 did not give good results, so this number of VGs was chosen for introducing its results. The value of *z/h* for runs case4a and case4b is the average vertical distance ratio, while in this case the VGs are placed at equal distances of *0.0939m* on the hull surface. All VGs defined in the previous table were set normally to the hull form and located at the same distance from the beginning of the high pressure region on the hull form. However, the effect of varying the distance between the trailing edges of the VGs and the beginning of the high pressure zone ($\Delta X_{VG}/h$) has been investigated in this study, as will be discussed latter.

4.0 COMPUTATIONAL DETAILS

The computational domain has been chosen to be a quarter of an elliptical cylinder, as shown in Fig. 3. It stretches out for half the ship's length in front of the ship hull, 1.5 times the ship's length behind the hull, one ship's length on the side and half the ship's length under the still water surface. The main axis *x*, *y*, *z*, represent the *streamwise*, *lateral* and *normaldirections*, respectively, as shown in Fig. 3. The unstructural tetrahedral grids have been used for meshing the computational domain using ICEM CFD software. The grids are concentrated on the VGs and on hull form of the ship model, especially at bow and stern regions (Fig. 4). Different sizes of mesh grids have been used to study the impact of the grid sizes on the results. The same sizes of mesh elements and number of mesh layers have been used on the ship hull form for the different runs of coarsen grids and finer grids (more mesh layers have been used with runs of finer grids) to insure good comparisons between the different runs. The different number of grids used in this study can be seen in Table 4.

The discretisation process has been made by applying the finite volume method. The high resolution advection scheme [12] has been used for discretizing the convective terms to prevent solution divergent, and first order upwind advection scheme has been used for the turbulence equations. The pressure is interpolated using linear interpolation scheme, while the velocity is interpolated using the trilinear scheme [12].

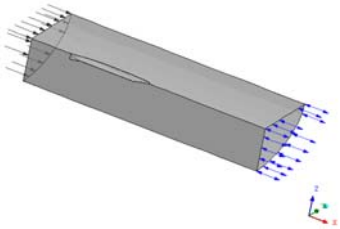

Figure 3: CFX computational domain for DTMB 5415 unit.

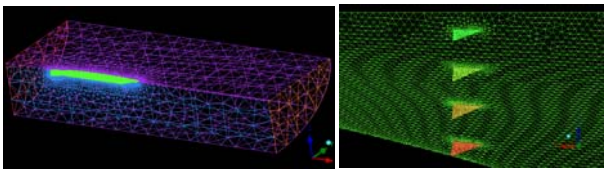

Figure 4 Numerical grids for the hull form of the DTMB 5415 unit. Left: the grids for the domain and the hull form without VGs (finer grids), right: the grids on the hull and VGs.

Table 4: Number of mesh elements used for every run.

Case	No. of elements	Case	No. of elements
case1a	402280	case3b	1338943
case1b	653949	case4a	432644
case2a	603881	case4b	1340182
case2b	2327195	case5a	637030
case3a	432159	case5b	2363059

5.0 RESULTS AND COMPARISONS

Fig. 5 gives comparisons between the experimental and the numerical values of C_{PV}, C_F and C_V of the different runs in this study, which can be considered as a first criterion for assessing the effect of the VGs on the ship viscous flow. Furthermore, Figs. 6 and 7 give comparisons between reduction or increase ratios in the ship viscous resistance components with respect to the resistance components of runs *case1a* and *case1b* due to the use of VGs, which give more clear indications about the effects of the VGs on the ship hull form viscous resistance.

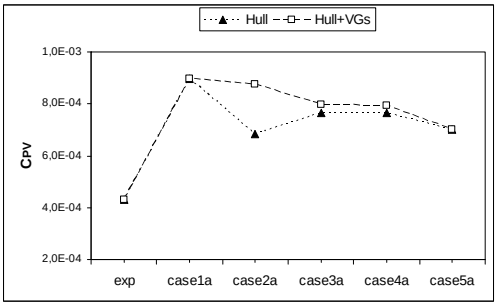

Figure 5(a) C_{PV} for coarsen grids runs

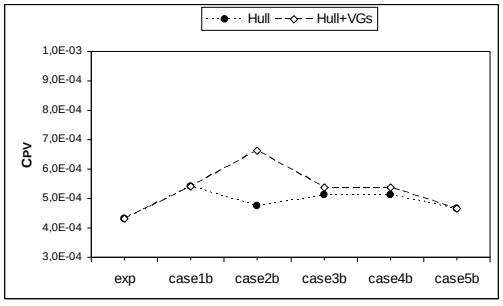

Figure 5(b) C_{PV} for finer grids runs

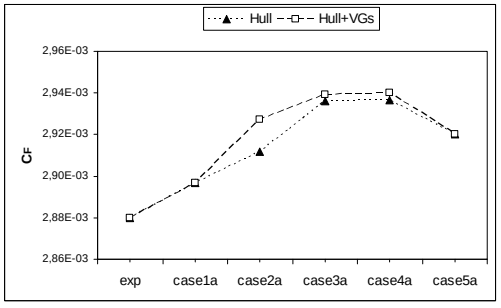

Figure 5(c) C_F for coarsen grids runs

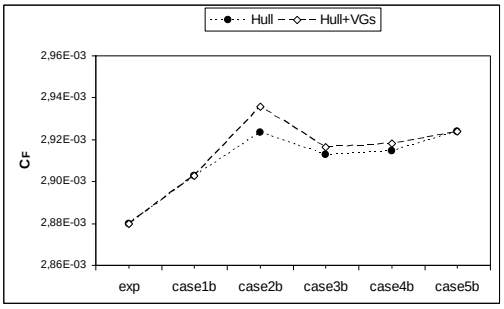

Figure 5(d) C_F for finer grids runs.

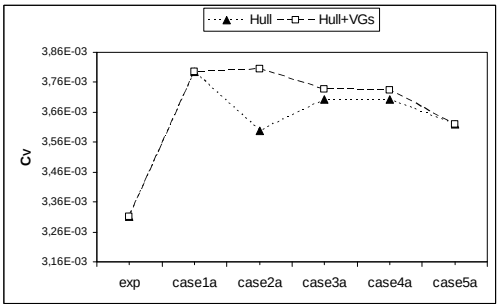

Figure 5(e) C_V for coarsen grids runs.

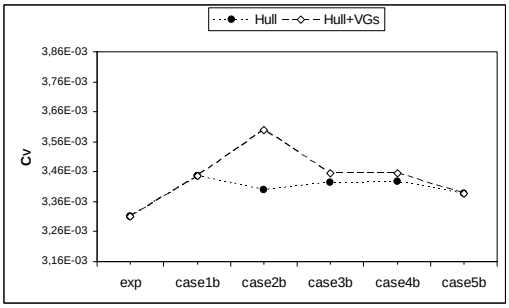

Figure 5(f) C_V for finer grids runs.

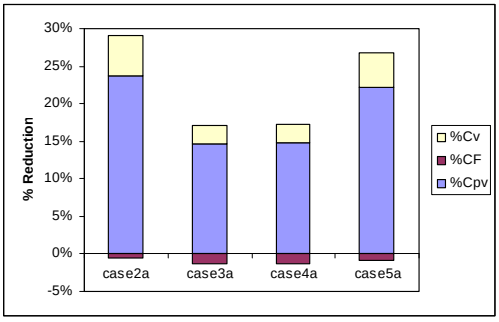

Fig. 6(a) results of hull

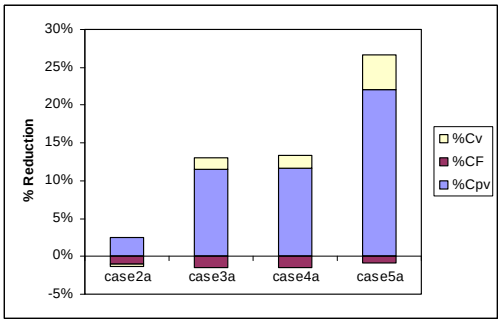

Fig. 6(b) results of hull + VGs

Figure 6: Percentage reduction in the value of C_V and its components for runs of coarsen grids, referred to the values of runs case1a and case1b respectively.

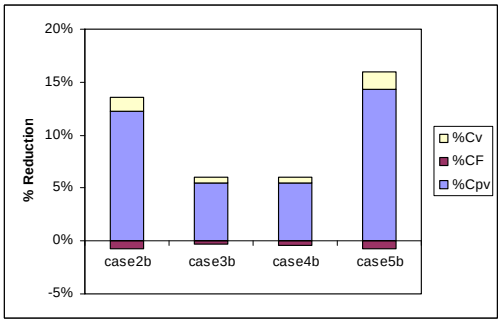

Fig. 7(a) results of hull.

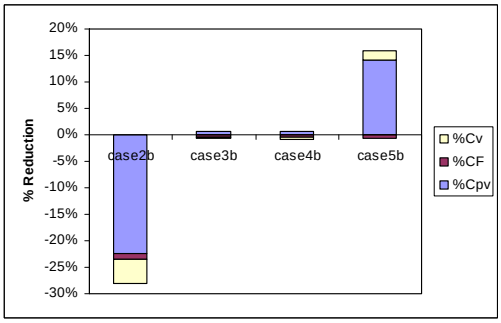

Fig. 7(b) results of hull + VGs.

Figure 7 Percentage reduction in the value of C_V and its components for runs of finer grids, referred to the values of runs case1a and case1b respectively.

It is well seen from Figs. 5(a) and 5(b) the reduction that occurred to the hull formC_{PV} due to the effect of increasing the fluid velocity in the ship boundary layer originated from the effect of VGs. The figures also show the use of VGs with higher size ($h/\delta \approx 0.2$) may lead to higher reduction in the hull C_{PV}, in comparison with the VGs of lower size. This off course refers to the strong vortices generated by these types of VGs. However, the effect of using VGs with higher size may lead to nearly very small reduction in the value of total C_{PV} (C_{PV} of the hull + C_{PV} *of* VGs), as shown in Fig. 6(b) (the reduction ratio is 2.47%), which makes the use of VGs with lower size ($h/\delta \approx 0.1$) is probably better. The runs of finer grids confirm this deduction, but show an adverse increase in the total value of C_{PV} for run case2b, as shown in Fig. 7(b). This may refer to the complicated fluid structure generated in this case, which require more finer grids and may even more accurate turbulence model for investigating such case. In general, the use of VGs of slots type show very good effect in the value of the ship viscous pressure resistance and the total value of this resistance component with the coarsen and finer grids runs, as can be seen from Figs. 5, 6 and 7.

Fig. 8 shows the pressure distribution in the aft region of the ship hull for the cases with and without VGs. The figure shows the region of high pressure (low velocity region, where the flow separation occurs) is expanded in the aft direction due to the effect of VGs, which reduce the effect of the flow separation in this region and this in turn reduces the viscous pressure resistance of the hull form. However, the high pressure distribution around the VGs of the different runs shown in the previous figure indicates that the VGs themselves cause drag. The VGs of $h/\delta \approx 0.2$ seems to affect greatly on the zone of high pressure in comparison with other types, but unfortunately due to their size they may lead to an increase in the overall viscous resistance which means more ship resistance at the end. Generally, the modification in the velocity distribution in the ship aft part as a result of using VGs may lead to an improvement in the axial flow distribution in the propeller wake region, which will lead in turn to an improvement in the propulsive efficiency.

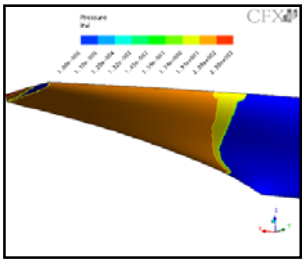

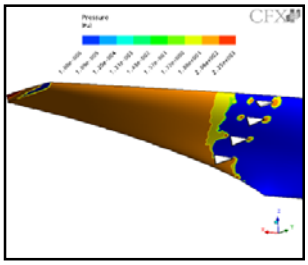

Figure 8(a) Case1b (without VGs)Figure 8(b) Case2b (with VGs)

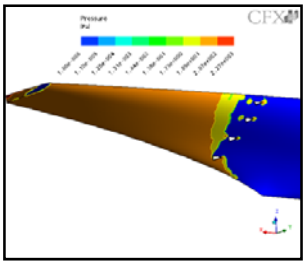

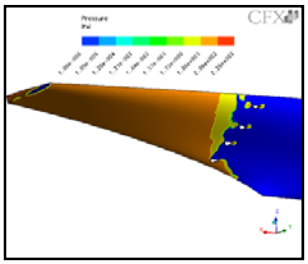

Figure 8(c) Case3b (with VGs) Figure 8(d) Case4b (with VGs)

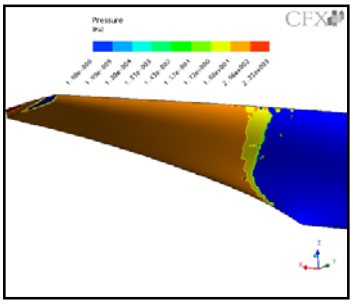

Figure 8(e) Case5b (with slots)

Figure 8: Pressure distribution on the ship aft part.

One of the main reasons for testing VGs with different sizes is the trial for choosing a device generates relatively strong vortices with small wetted surface area to reduce the effect of increasing the frictional resistance due to the addition of VGs. In general, the different devices used in this study did not lead to higher increase in the value of total frictional resistance coefficient, as can be seen from the results of the different runs in Figs. 5, 6 and 7, and the maximum increase in the value of C_F was nearly 1.5% of VGs with $h/\delta \approx 0.2$ which was expected due to their relatively higher wetted surface area.

The VGs of slots type show good reduction in the value of the total viscous resistance for the coarsen and finer grids runs and considered to be according to this study the best device with respect to the other types of VGs. Moreover, the VGs of $h/\delta \approx 0.1$ show some improvement in the value of total C_V as shown in Fig. 6(b), but this effect does not appear in the case of finer runs (Fig. 7(b)), which may refer to the insensitivity of the fluid solver for detecting the flow pattern correctly with finer grids runs. Figs. 5, 6 and 7 show that the results of runs case3a, case4a are approximately the same, which means the effect of the VGs on the boundary layer were nearly the same even with changing the distance between the devices. The same deduction can applied to the finer grids runs case3b and case4b.

Run case2b has been taken as an example for investigating the effect of varying the distance between the VGs and the beginning of high pressure zone, which represented by the parameter $\Delta X_{VG}/h$. The values of 16.4 and 9.4 have been intended for $\Delta X_{VG}/h$, in addition to the value of 2.4 of the original case. The effect of varying this parameter on the ship viscous resistance components and hence on the ship viscous resistance can be seen in Fig. 9 below. The results in the previous figure give the following indications:

I. The increase of $\Delta X_{VG}/h$ leads to lower increase in the hull frictional resistance or its total value.
II. The value of C_{PV} of the hull and for the hull plus VGs improved with the more decrease of $\Delta X_{VG}/h$ value.
III. The viscous resistance is affected by varying $\Delta X_{VG}/h$ which may become bigger than the original value of the hull form without VGs. This means the location of VGs need some kind of optimization to reach to the most favorable value of $\Delta X_{VG}/h$ which lead to the better results.

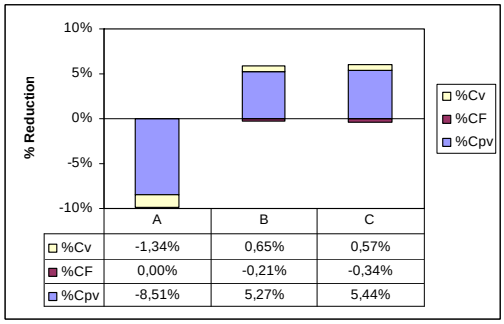

Fig. 9(a) viscous resistance components for the hull form only, right

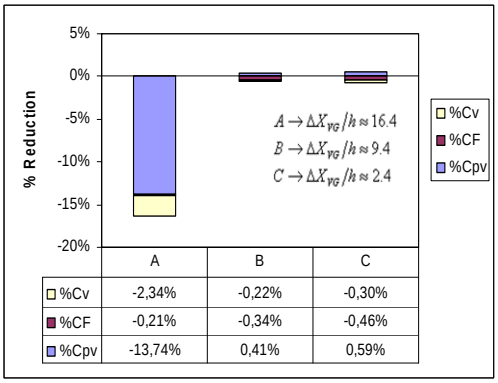

Fig. 9(b): viscous resistance components for the hull from plus the resistance components of VGs.

Figure 9: The effect of varying $\Delta X_{VG}/h$ parameter on the ship viscous resistance.

6.0 CONCLUSIONS

Numerical simulations for the viscous flow around a ship hull form with and without VGs using the commercial code Ansys CFX were carried out in this study. The obtained results showed generically the capability of the VGs on reducing ship viscous resistance component, but this may be accompanied by slightly increasing in the ship frictional resistance component. The resistance components of these VGs when added to the ship viscous resistance components this may lead to an increase in the total viscous resistance value. This give an important indication about the requirement of an optimization process for choosing the most suitable type of VGs required for a certain hull form. As well, it has been found that the final effect of the VGs on the ship viscous resistance will depend on: the type of VGs used, dimensions of VGs, number of VGs, the distance between the VGs trailing edges and the beginning of high pressure zone. However, experimental investigations are really

required in this field to obtain more clear picture and understanding about the actual effect of the VGs on the ship boundary layer separation and hence on the ship viscous resistance.

There were some differences between the results of the coarsen grids runs and the finer grids runs for detecting the effects of VGs on ship viscous resistance. In addition, the VGs of cylinder type has been tested also, but the results did not add to the results discussed in this paper due to the requirements of more investigations with this type of VGs, where the flow structure as well known is very complicated behind the cylinders at high Reynolds number. Generally, these may give indications of the requirement of further numerical investigations with: more finer grids, structural grids, transient simulations and more accurate turbulence models.

ACKNOWLEDGEMENTS

The authors would like to convey a great appreciation to the Faculties of Engineering in Universiti Teknologi Malaysia (UTM) and Alexandria University.

REFERENCES

1. Gad-el-Hak M., Bushnell D. (1991), Separation control: review, *Journal of Fluids Engineering*, Vol. 113, pp. 5-30.
2. Haines A.(1998), Know your flow: the key to better prediction and successful innovation, AIAA Paper 98-0221, *36th AIAA Aerospace Science Meeting and Exhibit*, Reno, NV, January 12-15.
3. Schubauer G., Spangenber W. (1960), Forced mixing in boundary layers, *Journal of Fluids Mechanics*, Vol. 8, pp. 10-32.
4. Calarese W., Grisler W., Gustsfson G. (1985), Afterbody drag reduction by vortex generators, AIAA Paper 85-0354, *AIAA 23rd Aerospace Science Meeting*, Reno, NV, January 14-17.
5. Kuethe A. (1972), Effect of streamwise vortices on wake properties associated with sound generation, *Journal of Aircraft*, Vol. 9, No. 10, pp.715-9.
6. John C. (2002), Review of research on low-profile vortex generators to control boundary layer separation, *Progress in Aerospace Sciences*, Vol. 38, pp. 389-420.
7. Oledal M. (1997), Application of vortex generators in ship propulsion system design, *ODRA 97' 2nd International Conference on Marine Technology*, Computational Mechanics Publications, pp. 247-25.
8. WebPage:http://www.iihr.uiowa.edu/gothenburg2000/5415 /combatant.html
9. Versteeg H., Malalasekera W. (1995), An Introduction to Computational Fluid Dynamics – The Finite Volume Method, Longman Group Ltd.
10. Godard G., Stanislas M. (2006), Control of decelerating boundary layer – part 1: optimization of passive vortex generators, *Aerospace Science and Tech*nology, Vol. 10, pp. 181-191.
11. Brandner P., Walker G. (2003) Hydrodynamic performance of a vortex generator, *Experimental Thermal and Fluid Science*, Vol. 27, pp. 573-582.
12. CFX User's Manual, Ansys CFX, 2013.